

## Far-infrared dielectric response and hopping conductivity in quasi-one-dimensional $(\text{NbSe}_4)_3\text{I}$

This article has been downloaded from IOPscience. Please scroll down to see the full text article.

1989 J. Phys.: Condens. Matter 1 10585

(<http://iopscience.iop.org/0953-8984/1/51/026>)

View [the table of contents for this issue](#), or go to the [journal homepage](#) for more

Download details:

IP Address: 129.252.86.83

The article was downloaded on 27/05/2010 at 11:14

Please note that [terms and conditions apply](#).

## Far-infrared dielectric response and hopping conductivity in quasi-one-dimensional $(\text{NbSe}_4)_3\text{I}$

V Zelezny†, J Petzelt†, B P Gorshunov‡, A A Volkov‡, G V Kozlov‡, P Monceau§ and F Levy||

† Institute of Physics, Czechoslovak Academy of Sciences, 18040 Prague 8, Na Slovance, 2, Czechoslovakia

‡ Institute of General Physics, Academy of Sciences of the USSR, Vavilov Street 38, 117942 Moscow, USSR

§ Centre de Recherches sur les Très Basses Températures, CNRS, BP 166 X, 38042 Grenoble Cédex, France

|| Institut de Physique Appliquée, Ecole Polytechnique Fédérale de Lausanne, Lausanne CH-1015, Switzerland

Received 17 July 1989, in final form 5 September 1989

**Abstract.** Complex transmittance of the quasi-one-dimensional semiconductor  $(\text{NbSe}_4)_3\text{I}$  in the  $8\text{--}30\text{ cm}^{-1}$  range and reflectivity in the  $15\text{--}650\text{ cm}^{-1}$  range were measured as a function of temperature ( $10\text{--}300\text{ K}$ ) around the structural phase transition at  $T_c = 274\text{ K}$ . The spectra show predominantly dielectric characters with a rich phonon structure between  $20$  and  $300\text{ cm}^{-1}$ . Several new lines gradually appear below  $T_c$  in qualitative agreement with the factor-group analysis. The submillimetre electronic conductivity along the chain direction is appreciably higher than the DC conductivity in the whole temperature range which suggests a hopping mechanism of the electron transport. This is even more directly documented by the strong increase in submillimetre permittivity with temperature. The important role of permittivity for proving the hopping transport is stressed.

### 1. Introduction

Infrared (IR) spectroscopy is a powerful technique in the study of phase transitions (Petzelt and Dvorak 1984); it has been used in particular in the case of anisotropic materials with one-dimensional (1D) or two-dimensional (2D) structures. These materials are known to be unstable against a lattice distortion and to undergo a Peierls (1955) transition between a high-temperature metallic state and a low-temperature charge-density wave (CDW) state of less conductivity or with a semiconducting state. In the last decade, such transitions have been found in many compounds such as 2D layered dichalcogenides (Wilson *et al* 1975), or 1D organic conductors (Devreese *et al* 1979), linear-chain platinum complexes, transition-metal trichalcogenides, molybdenum oxides and halogenated transition-metal tetrachalcogenides of general formula  $(\text{MSe}_4)_n\text{I}$  with  $\text{M} \equiv \text{Ta}$  or  $\text{Nb}$  (Monceau 1985, Caron and Jerome 1987). The 1D compounds have been intensively studied because of the spectacular dynamical properties of the CDW condensate which can be accounted for by the translational motion of the CDW ground state when it has been freed from impurity centres which pin it (Monceau 1985, Rouxel

1986, Grüner 1988, Schlenken 1989). In this respect, IR and far-IR measurements have yielded the Fröhlich effective mass of the condensate and allowed the determination of the CDW excitations (Gorshunov *et al* 1986) in tetrathiofulvalinium-tetracyanoquinodimethanide (TTF-TCNQ).

Compounds of the  $(MSe_4)_nI$  family consist of  $MSe_4$  chains parallel to the  $c$  axis separated from one another by iodine. Each metal atom is sandwiched by two rectangular selenium units. The dihedral angle between adjacent rectangles is about  $45^\circ$  so that the stacking unit in a chain is a  $[NbSe_8]$  rectangular anti-prism. According to the composition which varies the  $d_z^2$  band filling of the transition metal  $M$ , different structural and electrical properties occur: on the one hand,  $(TaSe_4)_2I$  and  $(NbSe_4)_{10}I_3$  undergo a Peierls transition at  $T_p = 263$  K (Wang *et al* 1983a) and 285 K (Wang *et al* 1983b), respectively, with, below  $T_p$ , non-linear transport properties and, on the other hand,  $(NbSe_4)_3I$  exhibits a ferrodistorptive structural phase transition at  $T_c = 274$  K (Gressier *et al* 1984, Izumi *et al* 1984a). For this latter compound the  $NbSe_4$  chain along  $c$  comprises six  $NbSe_4$  units in the unit cell and is strongly distorted above  $T_c$  with two long Nb–Nb distances of 3.25 Å and a short Nb–Nb distance of 3.06 Å (Meerschaut *et al* 1977). Below  $T_c$  the chains are less distorted with a Nb–Nb sequence of 3.31, 3.17 and 3.06 Å (Gressier *et al* 1985). This accounts for the semiconducting behaviour above  $T_c$  with an energy gap of 0.21 eV (defined from the temperature variation in the electrical resistivity following the law  $\rho(T) = \rho_0 \exp(-\Delta/kT)$  to a semiconducting state below  $T_c$  with a much smaller gap of 0.08 eV (Gressier *et al* 1984). At lower temperatures ( $T < 120$  K), different activation energies have been reported on different types of crystals: crystals of type I keeping the very low value for the gap measured just below  $T_c$  and crystals of type II for which the activation energy increases again to a value of 0.15 eV (Gressier *et al* 1984, Taguchi *et al* 1986). Up to now it has not been possible to determine the physical parameters which distinguish between these two types.

Structural analysis (Izumi *et al* 1984b) of the two phases of  $(NbSe_4)_3I$  above and below  $T_c$  shows that the phase transition is ferrodistorptive but non-ferroelectric and non-ferroelastic. The space group change is  $P4/mnc \rightarrow P\bar{4}2_1c$  without a change in the number of formula units in the unit cell ( $Z = 4$ ). The order parameter is of  $B_{1u}$  symmetry and the corresponding soft mode, which above  $T_c$  is a silent (IR- and Raman-inactive) zone-centre mode, was observed below  $T_c$  in Raman spectra (Sekine *et al* 1984). Recently, the softening of the  $c_{44}$  elastic stiffness below  $T_c$  has been studied by ultrasonic measurements (Saint-Paul *et al* 1988) and the dispersion of acoustic branches have been measured by inelastic neutron scattering (Monceau *et al* 1989). The phase transition has also been studied by x-ray diffraction (Iwazumi *et al* 1986), electron diffraction (Roucau *et al* 1984), specific heat (Smontara *et al* 1986, 1987) and transport measurements (Smontara *et al* 1987, Gressier *et al* 1984, Taguchi *et al* 1986, Izumi *et al* 1984a) and NMR techniques (Butaud 1985).

Moreover, it has been reported that another phase transition may take place near 90 K (Izumi *et al* 1987) into a phase with the space group  $P\bar{4}$  ( $Z = 4$ ) according to the observation of new x-ray Bragg reflections forbidden in the  $P\bar{4}2_1c$  group. The corresponding soft mode is again a silent mode of  $A_2$  symmetry in the  $P\bar{4}2_1c$  phase which should become Raman active in the  $P\bar{4}$  phase. A weak mode showing partial softening which disappears above about 100 K was actually observed in  $a'(cc)\bar{a}'$  Raman spectra (Sekine *et al* 1987). However, it should be noted that recent neutron scattering experiments (Currat and Bernard 1989) give no support to the existence of this phase transition so that its existence is still questionable.

In this paper, we report the IR and submillimetre transmission measurements of  $(NbSe_4)_3I$  from room temperature down to 10 K. So far only qualitative reflectivity

measurements carried out on non-ideal mosaic samples have been published (Izumi *et al* 1984a, 1987). The progress in crystal growth and submillimetre spectroscopy allowed us to perform quantitative measurements, enabling evaluation of the dielectric response and conductivity spectra in this substance.

## 2. Experimental details

Two mosaic samples consisting of a few polished single-crystal platelets were prepared: a smaller sample for transmission measurements with area of about  $0.3 \text{ cm}^2$  and thickness  $142 \mu\text{m}$  and a thicker sample of the same size for reflectivity measurements.

The transmission measurements in the  $8\text{--}30 \text{ cm}^{-1}$  range were performed using a self-made quasi-optical Epsilon spectrometer based on tunable monochromatic backward-wave-oscillator sources (Volkov *et al* 1985). In this technique, the intensity and phase of the radiation transmitted through the plane parallel plate are usually measured using a Mach–Zehnder interferometer and the spectra of complex dielectric function  $\hat{\epsilon}(\nu) = \epsilon'(\nu) - i\epsilon''(\nu)$  are directly calculated using standard formulae. The accuracy of this method is much higher than that of the usual reflectivity measurements.

The reflectivity spectra were measured using a Bruker IFS 113v Fourier transform interferometer with a Ge bolometer for the  $15\text{--}100 \text{ cm}^{-1}$  range and standard pyroelectric detector for the  $50\text{--}650 \text{ cm}^{-1}$  range. The sample was stuck on a cold finger of an Oxford Instrument CF 104 continuous-flow cryostat in vacuum.

## 3. Results and evaluation

In figure 1 we show the  $E \parallel c$  and  $E \perp c$  room-temperature reflectivity spectra of  $(\text{NbSe}_4)_3\text{I}$ . No appreciable structure is seen above  $400 \text{ cm}^{-1}$  so that we do not show this part of the spectra. The temperature dependence was investigated only for the  $E \parallel c$  polarisation which is expected to be more informative. The results for some selected temperatures are presented in figure 2. The reflectivities at 300 and 80 K were analysed by Kramers–Kronig relations to obtain the complex dielectric functions. Outside the measured spectral range the reflectivity was extrapolated by a constant. The calculated real and imaginary parts of permittivity are shown in figures 3 and 4, respectively. Below  $30 \text{ cm}^{-1}$ , the more accurate values of  $\epsilon'(\nu)$  and  $\epsilon''(\nu)$  obtained directly from transmission measurements (Epsilon spectrometer) are shown. This part is shown in more detail in figure 5. Reasonable agreement between both types of experiment is found. In figure 6 we show the analogous spectra for  $E \perp c$  polarisation. The low-frequency behaviour at  $11 \text{ cm}^{-1}$  as a function of temperature is shown in figure 7.

All the mode frequencies evaluated from maxima of the  $\epsilon''(\nu)$  spectra (corrected for not very high damping) are listed in table 1. The  $20 \text{ cm}^{-1}$  mode parameters were evaluated by fitting the transmittance spectra to a model of a classical oscillator plus a Drude term to account for the absorption background (see broken lines in figure 5). The magnitude of the background for each temperature was determined from direct evaluation of the  $\epsilon'(\nu)$  and  $\epsilon''(\nu)$  spectra near 10 and  $30 \text{ cm}^{-1}$  where the sample is more transparent (bold lines in figure 5). The temperature dependence of the oscillator parameters is shown in figure 8. The temperature dependence of the conductivity  $\sigma(\nu) = (\nu/60) \epsilon''(\nu) (\Omega^{-1} \text{ cm}^{-1})$  at 8 and  $30 \text{ cm}^{-1}$  and permittivity at  $30 \text{ cm}^{-1}$  are shown in figure 9 where the DC conductivity is added for comparison (Izumi *et al* 1984a).

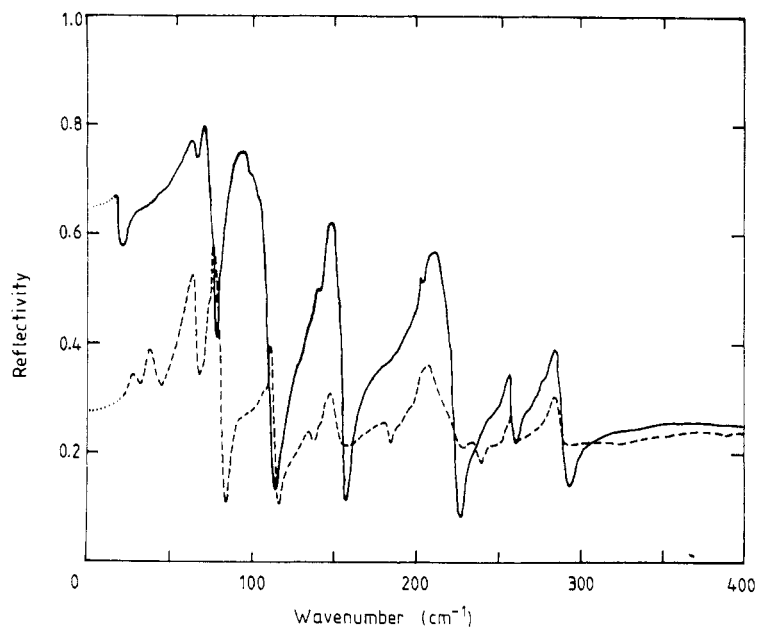


**Figure 1.** Far-IR reflectivities of  $(\text{NbSe}_4)_3\text{I}$  at 300 K for the ordinary ( $E \perp c$ ) (—) and extraordinary ( $E \parallel c$ ) (---) ray.

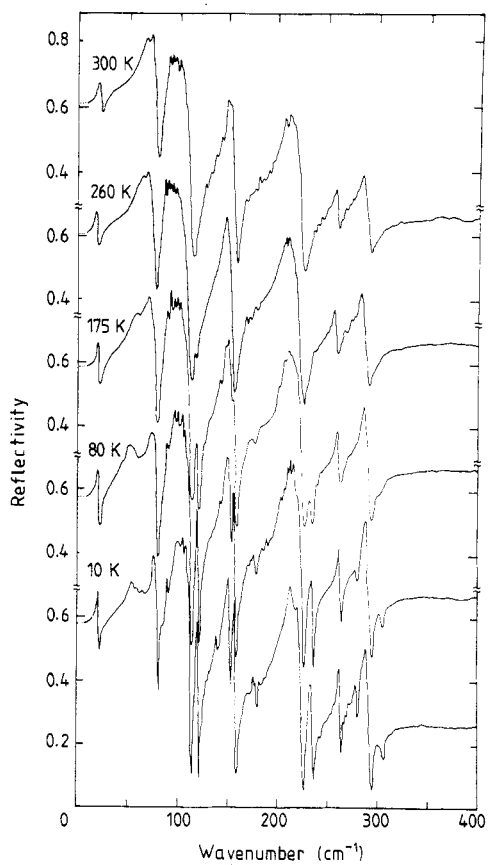


**Figure 2.** Temperature dependence of the  $E \parallel c$  reflectivity of  $(\text{NbSe}_4)_3\text{I}$ .

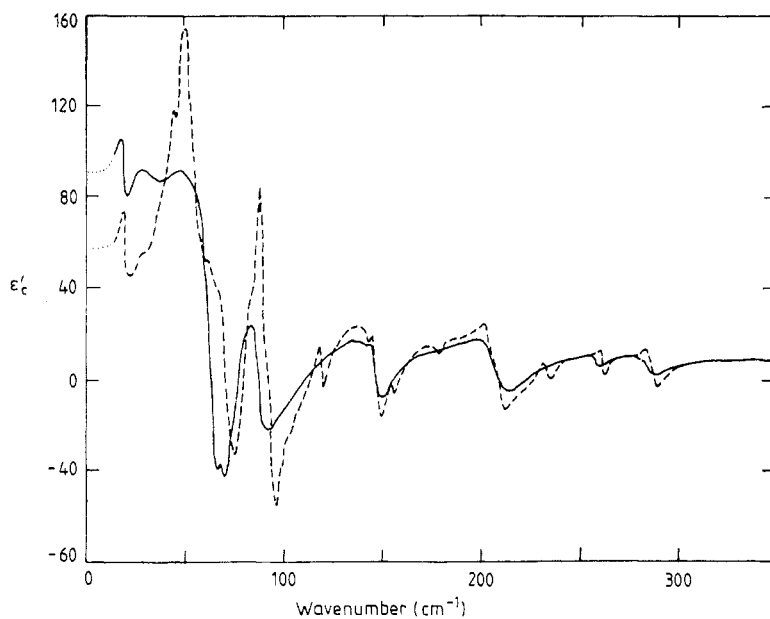


**Figure 3.** Real part of the  $\epsilon_c$  permittivity spectra of  $(\text{NbSe}_4)_3\text{I}$  at 300 K (—) and 80 K (---).

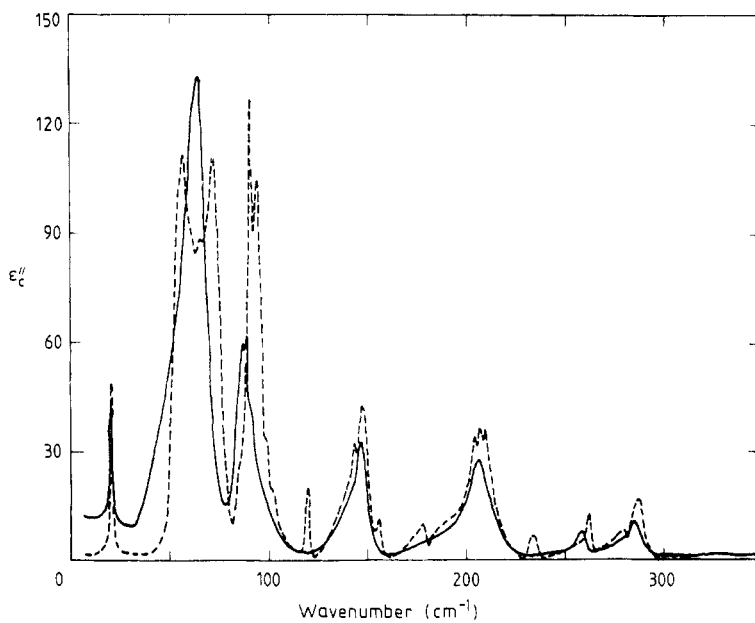


**Figure 4.** Imaginary part of the  $\epsilon_c$  spectra of  $(\text{NbSe}_4)_3\text{I}$  at 300 K (—) and 80 K (---).

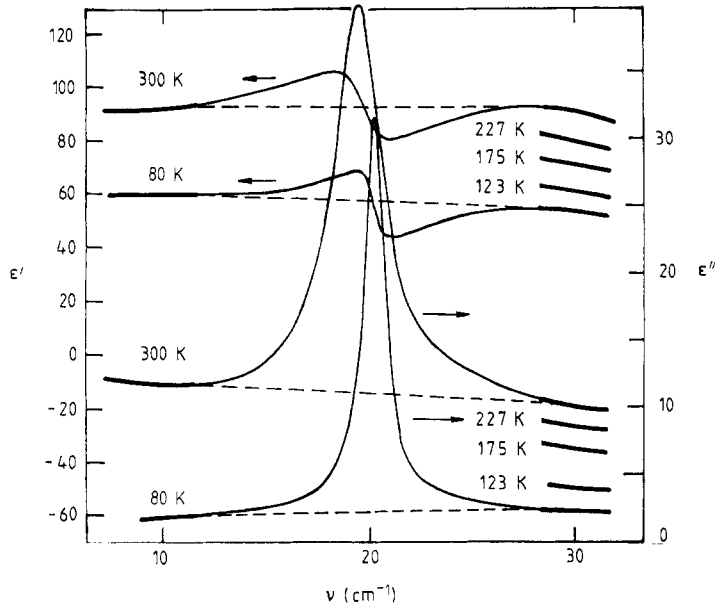


Figure 5. Complex submillimetre permittivity spectra of  $(\text{NbSe}_4)_3\text{I}$  for  $E \parallel c$ .

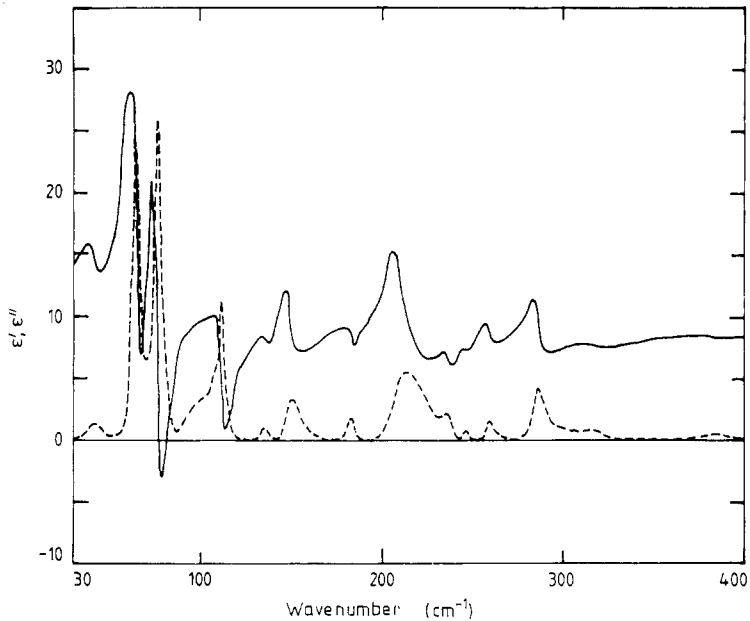


Figure 6. Complex far-IR permittivity of  $(\text{NbSe}_4)_3\text{I}$  at 300 K for  $E \perp c$ : —,  $\epsilon'$ ; ---,  $\epsilon''$ .

#### 4. Discussion

All the spectra show predominantly phonon absorption. The  $E \parallel c$  spectra are in agreement with previous qualitative measurements by Izumi *et al* (1984a, 1987). The plasma

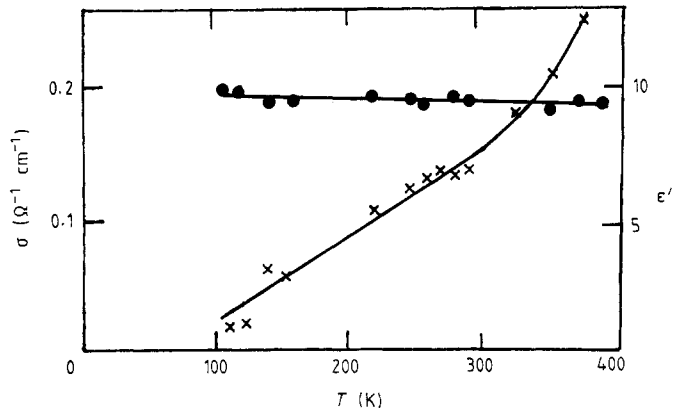


Figure 7. Temperature dependence of the submillimetre conductivity ( $\times$ ) and permittivity ( $\bullet$ ) of  $(\text{NbSe}_4)_3\text{I}$  for  $E \perp c$  ( $\nu = 11 \text{ cm}^{-1}$ ).

edge of the free carriers is hidden in the stronger phonon reststrahl bands and is probably overdamped.

The number of phonon modes can be compared with the group theoretical prediction. In table 2 we bring the results of factor-group analysis in all three phases using the structural data of Meerschaut *et al* (1977) and the tables of Rousseau *et al* (1981). The results for the high-temperature phase agree with those of Sekine *et al* (1984). We can see that the number of IR-active modes (ten and 21  $E \parallel c$  modes for the high- and low-temperature phases, respectively, and 27 modes for  $E \perp c$ ) is in qualitative agreement with table 2. All the modes lie below  $400 \text{ cm}^{-1}$ , so that simplifying decomposition into higher-frequency  $\text{NbSe}_4$  internal modes and lower-frequency external modes seems to be meaningless. Concerning IR selection rules, the suggested low-temperature phase with  $P4$  space group does not differ from the phase with  $P4_21c$  space group so that no conclusion concerning the existence of the second phase transition can be made from our data.

The absorption background in figure 5 gives evidence of some free-carrier absorption in the submillimetre range. The corresponding submillimetre conductivity is higher than the DC conductivity (see figure 9) which gives evidence of a hopping mechanism for the conductivity in this compound. The strong increase in  $\epsilon'$  in the submillimetre range with increasing temperature is in agreement with the increasing  $\sigma(\nu)$  spectrum (via Kramers-Kronig relations). The graphical estimate of phonon strength from figure 4 shows that the low-frequency value  $\epsilon'_c(80 \text{ K}) = 60$  is entirely due to higher-frequency phonon contributions  $\epsilon_L \approx 50$  and optical electronic processes  $\epsilon_\infty \approx 10$ ,  $\epsilon'_c(80 \text{ K}) = \epsilon_L(80 \text{ K}) + \epsilon_\infty(80 \text{ K})$ . However, these contributions are almost temperature independent so that the increase in  $\epsilon'_c$  to the value  $\epsilon'_c(300 \text{ K}) = 90$  (see also figures 5 and 9) must be caused by the contribution from conduction electrons. Such a spectral behaviour is not described by the classical Drude model. The Drude model leads to a slight negative contribution to the static permittivity which relaxes in the same frequency range where the Drude conductivity decreases to zero (i.e. near the plasma damping frequency  $\Gamma$ ). On the other hand, hopping conductivity which is typical of band conductors, unlike the Drude model, has  $\sigma(\nu)$  which increases with increasing  $\nu$  typically in the microwave range and in this way leads to strong positive contribution to static permittivity (Barker *et al* 1976). This



**Table 1.** Transverse polar phonon mode frequencies in (NbSe<sub>4</sub>)<sub>3</sub>I.

| Polarisation         | Temperature                     |    |      |    |    |    |     |     |     |     |     |     |     |     |     |     |     |     |     |     |     |     |
|----------------------|---------------------------------|----|------|----|----|----|-----|-----|-----|-----|-----|-----|-----|-----|-----|-----|-----|-----|-----|-----|-----|-----|
|                      | Frequencies (cm <sup>-1</sup> ) |    |      |    |    |    |     |     |     |     |     |     |     |     |     |     |     |     |     |     |     |     |
| <i>E</i>    <i>c</i> | 80                              | 80 | 55   | 70 | 89 | 93 | 119 | 143 | 146 | 155 | 177 | 186 | 190 | 203 | 206 | 209 | 233 | 252 | 261 | 278 | 287 | 304 |
| <i>E</i> ⊥ <i>c</i>  | 300                             |    | 19.6 | 63 | 87 |    |     | 146 |     |     |     |     |     | 206 |     |     |     | 257 |     |     | 284 |     |
| <i>E</i> ⊥ <i>c</i>  | 300                             |    | 41   | 64 | 77 | 97 | 107 | 111 | 136 | 150 | 183 | 213 | 236 | 246 | 260 | 286 | 318 | 385 |     |     |     |     |

**Table 2.** Factor-group analysis of long-wavelength lattice vibrations in all phases of (NbSe<sub>4</sub>)<sub>3</sub>I.  $\alpha_{ii}$  ( $i = x, y, z$ ) denotes the allowed Raman tensor components (Raman activity) and  $e_i$  the allowed effective charge components (IR activity).

| P4/mnc(D <sub>4h</sub> <sup>1</sup> ), Z = 4 |                 |  | P4 <sub>2</sub> /c(D <sub>2d</sub> <sup>1</sup> ), Z = 4 |                 |  | P4(S <sub>4</sub> ), Z = 4 |                 |  |
|--|-----------------|--|--|-----------------|--|----------------------------|-----------------|--|
| Species                                      | Number of modes | Activity                                 | Species  | Number of modes | Activity                                     | Species                    | Number of modes | Activity                                     |
| A <sub>1g</sub>                              | 12              | $\alpha_{xx} + \alpha_{yy}, \alpha_{zz}$ | A <sub>1</sub>   | 22              | $\alpha_{xx} + \alpha_{yy}, \alpha_{zz}$     | A                          | 44              | $\alpha_{xx} + \alpha_{yy}, \alpha_{zz}$     |
| B <sub>1u</sub>                              | 10              | —  | A <sub>2</sub>   | 22              | —  |                            |                 |  |
| A <sub>2g</sub>                              | 13              | —  | B <sub>2</sub>   | 22              | $\alpha_{xy}, e_z$                           | B                          | 22              | $\alpha_{xy}, e_z$                           |
| B <sub>2u</sub>                              | 9               | —  | E  | 52              | $(\alpha_{xz}, \alpha_{yz})$<br>$(e_x, e_y)$ | E                          | 52              | $(\alpha_{xz}, \alpha_{yz})$<br>$(e_x, e_y)$ |
| A <sub>2u</sub>                              | 11              | $e_z$                                    |  |                 |  |                            |                 |  |
| B <sub>2g</sub>                              | 11              | $\alpha_{xy}$                            |  |                 |  |                            |                 |  |
| E <sub>g</sub>                               | 24              | $(\alpha_{xz}, \alpha_{yz})$             |  |                 |  |                            |                 |  |
| E <sub>u</sub>                               | 28              | $(e_x, e_y)$                             |  |                 |  |                            |                 |  |

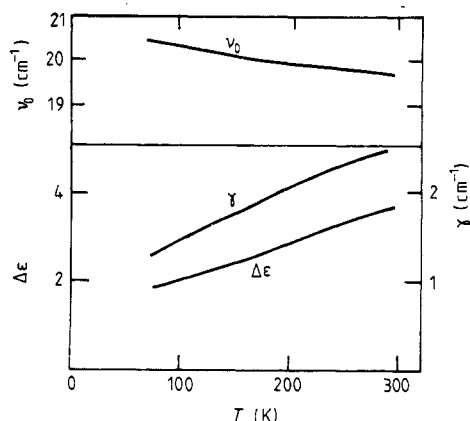


Figure 8. Temperature dependence of the classical oscillator parameters of the submillimetre  $A_{2u}$  ( $B_2$ ) mode of  $(\text{NbSe}_4)_3\text{I}$  for  $E \parallel c$ .

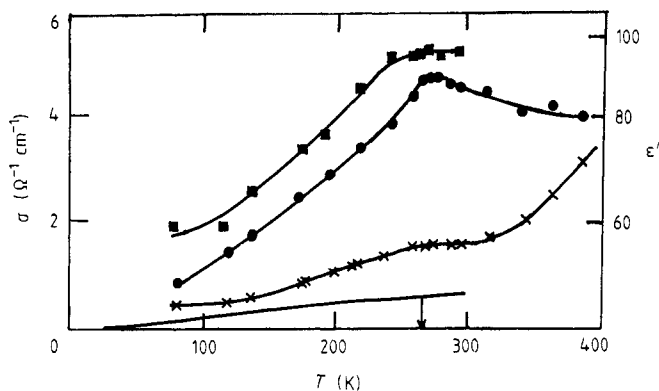


Figure 9. Temperature dependence of the submillimetre conductivity  $\sigma$  (—, at  $0 \text{ cm}^{-1}$ ;  $\times$ , at  $8 \text{ cm}^{-1}$ ;  $\blacksquare$ , at  $30 \text{ cm}^{-1}$ ) and permittivity  $\epsilon'$  (at  $30 \text{ cm}^{-1}$ ) ( $\bullet$ ) of  $(\text{NbSe}_4)_3\text{I}$  for  $E \parallel c$ .

is in complete agreement with the behaviour of  $(\text{NbSe}_4)_3\text{I}$  for  $E \parallel c$ . We note that the behaviour of  $\epsilon'(\nu)$  is much more sensitive to the hopping mechanism than the conductivity spectrum itself and therefore we stress the importance of its experimental determination in semiconducting systems; this has not been generally appreciated so far.

Finally, let us comment on the  $E \perp c$  response (figures 6 and 7). The submillimetre conductivity and permittivity are much lower than for the  $E \parallel c$  polarisation. The lower conductivity is in agreement with its 1D character; the lower permittivity shows that the effective charges of polar phonons are weaker than for the  $E \parallel c$  polarisation. It seems that it is caused by stronger electron-phonon coupling in the  $E \parallel c$  polarisation whose microscopic origin needs closer investigation. Also the microscopic mechanism of the hopping conductivity between  $d_{z^2}$  orbitals of Nb atoms needs further study.

In conclusion, contrary to other more conducting 1D conductors, far-IR spectra in  $(\text{NbSe}_4)_3\text{I}$  are dominated by one-phonon absorption as in dielectrics. However, unlike the situation in dielectrics the hopping conductivity in the submillimetre range is connected by a strong additional positive contribution to the permittivity.

**References**

- Barker A S Jr, Ditzenberger J A and Remeika J P 1976 *Phys. Rev. B* **14** 4254
- Butaud P, Segransan P, Berthier C and Meerschaut A 1985 *Springer Lecture Notes in Physics* vol 217, ed. G Hutiray and J Solyom (Berlin: Springer) p 121
- Caron J and Jerome D 1987 *Low-Dimensional Conductors and Superconductors* vol 155 (New York: Plenum)
- Curat R and Bernard L 1989 private communication
- Devreese J T, Evrard R P and Van Doren V E 1979 *Highly Conducting One-Dimensional Solids* (New York: Plenum)
- Gorshunov B P, Kozlov G V, Volkov A A, Zelezny V, Petzelt J and Jacobsen C S 1986 *Solid State Commun.* **60** 681
- Gressier P, Guemas L and Meerschaut A 1985 *Mater. Res. Bull.* **20** 539
- Gressier P, Meerschaut A, Guemas L, Rouxel J and Monceau P 1984 *J. Solid State Chem.* **51** 141
- Grüner G 1988 *Rev. Mod. Phys.* **60** 1129
- Iwazumi T, Izumi M, Sasaki F, Yoshizaki R and Matsuura E 1986 *Physica B* **143** 261
- Izumi M, Iwazumi T, Seino T, Sekine T, Matsuura E, Uchinokura K and Yoshizaki R 1987 *Synth. Met.* **19** 863
- Izumi M, Iwazumi T, Seino T, Uchinokura K, Yoshizaki R and Matsuura E 1984a *Solid State Commun.* **49** 423
- Izumi M, Toshiaki T, Uchinokura K, Yoshizaki R and Matsuura E 1984b *Solid State Commun.* **51** 191
- Meerschaut A, Palvadeau P and Rouxel J 1977 *J. Solid State Chem.* **20** 21
- Monceau P 1985 *Electronic Properties of Inorganic Quasi One-dimensional Compounds*, Parts I and II, (Dordrecht: Reidel)
- Monceau P, Bernard L, Curat R and Levy F 1989 *Physica B* **156**–7 20
- Peierls R F 1955 *Quantum Theory of Solids* (London: OUP) p 108
- Petzelt J and Dvorak V 1984 *Vibrational Spectroscopy of Phase Transitions*, ed. Z Igbal and F J Owens (New York: Academic) p 56
- Roucau C, Ayrolles R, Gressier P and Meerschaut A 1984 *J. Phys. C: Solid State Phys.* **17** 2993
- Rousseau D L, Bauman R P and Porto S P S 1981 *J. Raman Spectrosc.* **10** 253
- Rouxel J 1986 *Crystal Chemistry and Properties of Materials with Quasi-one-dimensional Properties* (Dordrecht: Reidel)
- Saint-Paul M, Monceau P and Levy F 1988 *Phys. Rev. B* **37** 1024
- Schlenker C 1989 *Low-dimensional Electronic Properties of Molybdenum Bronzes and Oxides* (Dordrecht: Reidel)
- Sekine T, Izumi M and Matsuura E 1987 *Synth. Met.* **19** 869
- Sekine T, Uchinokura K, Izumi M and Matsuura E 1984 *Solid State Commun.* **52** 379
- Smontara A, Biljakovic K, Forro L and Levy F 1986 *Physica B* **143** 264
- 1987 *Synth. Met.* **19** 859
- Taguchi I, Levy F and Berger H 1986 *Physica B* **143** 258
- Volkov A A, Goncharov Yu G, Kozlov G V, Lebedev S P and Prokhorov A M 1985 *Infrared Phys.* **25** 369
- Wang Z Z, Monceau P, Renard M, Gressier P, Guemas L and Meerschaut A 1983b *Solid State Commun.* **47** 439
- Wang Z Z, Saint-Lager M C, Monceau P, Renard M, Gressier P, Meerschaut A, Guemas L and Rouxel J 1983a *Solid State Commun.* **46** 325
- Wilson J A, Di Salvo F J and Mahajan S 1975 *Adv. Phys.* **24** 117